Fractal Analysis of Light Scattering Data from Gravity-Driven Granular Flows

Ram Chand[1], Saeeduddin[2], Murad Ali Khaskheli[3], Abdul Majid Soomro[3], Hussain Saleem[4*], Waseem Ahmed Bhutto[3], Altaf H. Nizamani[3], Muhammad Yousuf Soomro[3], Nek Muhammad Shaikh[3], Sithi V. Muniandy[5]

[1]Department of Physics, College of Science, University of Hail, Hail 81451, Kingdom of Saudi Arabia.
[2]Centre of Excellence in Analytical Chemistry, University of Sindh, Jamshoro, Pakistan.
[3]Institute of Physics, University of Sindh, Jamshoro, Pakistan.
[4]Department of Computer Science, UBIT, University of Karachi, Karachi, Pakistan.
[5]Department of Physics, Faculty of Science, University of Malaya, 50603, Kuala Lumpur, Malaysia.
**Corresponding Author: hussainsaleem@uok.edu.pk*

Abstract
Fractal analysis is useful for studying complex fluctuation phenomena that exhibit scaling behavior. In this work, fractal analysis is used to characterize transient dynamics of gravity-driven surface granular flow down inclined plane. Intensity fluctuation of light scattered from granular flow is modelled by multifractional Brownian motion with time-varying Hurst exponent. Temporal variations in the Hurst exponents over the time-development of flow are analyzed for different particle sizes and opening sizes of the hopper.

Key words:
Dynamic Light Scattering (DLS), Fractal analysis, Granular flow, Multifractional Brownian Motion (MBM);

1. Introduction

Understanding the dynamics of granular flow helps us to understand the natural phenomena such as land-slides, blockage of rivers due to mud flow, snow avalanches etc. [1][2][3]. In addition to these natural phenomena, there are many engineering systems which involve granular flows [4][5]. These flows can be categorized in three dynamical states such as dilute or rapid flow (gas-like), dense or slow flow (fluid-like), and the jammed (solid-like) state [6]. Structural (flow) phase transition among the flow regimes can be explained by the Savage Number [7][8]. Grains contacts and frictional forces are generally used to describe these transitions [9][10]. Mostly, a dilute granular flow will evolve to dense flow, and finally to the jammed state due to energy dissipation through inelastic collisions and friction [11]. These phase transitions have fascinated granular scientists since the last two decades or so [12]. Particularly, the intermediate flow regimes of transitional flows are still not well understood [9].

For lower frictional base, the flow is approximately two-dimensional [13][14][15] and this termed as surface granular flow which is the case considered in this work. There occur many natural and man-made surface granular flow phenomena such as the luggage flow on conveyor belts, the transport of bottles in factories, traffic jam in a city, etc. [16].

Nevertheless, there have been relatively few studies reported on surface granular flow, particularly for gravity-driven $2D$ flows. Drake and his co-workers measured velocity and density profiles of granular flow down narrow $2D$ channels [16][17]. Similar measurements were also carried out in another study and the authors explained their results with prediction from a kinetic theory [18].

Recently, Yang $et\ al.$ have examined the structural phase transition of granular flows down a chute using DEM simulations [11]. In quasi-$2D$ granular channels, Zhong $et\ al.$ have investigated the transition from dilute to dense flow [8]. The dilute to dense transition depends on the global properties of channel, while that of dense to jammed state depends only on the ratio of size of hopper opening to particle size [14][19]. In spite of these studies, a very little is known about how the transition in flow occurs. There is not even a quantitative explanation of such transition and fluctuation of particles density.

Even though previous studies have concluded that controlling parameters such as hopper opening, particle size, inclination angle etc. are responsible for transition to occur, a general theory of the granular flows is still lacking [20]. Difficulty in modeling such an equation arises partially from the fact that sharp boundary between two regimes during transition is not examined carefully. One of the difficulties is that the velocity fluctuations at short time scale in these complex flows is difficult to measure. Dynamic light scattering (DLS) techniques have provided powerful tools to probe temporal dynamics which can corroborated with particle visualization and velocimetry analysis [21][22]. In DLS, coherent light beams are scattered by moving particles resulting in fluctuation in the interference patterns, also known as speckles. One can then extract useful transport characteristics by analyzing the light intensity fluctuation. DLS have been used for determining particle transport mechanisms and structural phase transition in complex dusty plasmas [23]. Menon $et\ al.$ [22] used Diffusive-Wave Spectroscopy to probe the interior dynamics of $3D$ flow of sand, which is difficult to study otherwise. Light scattering

Manuscript received July 5, 2019
Manuscript revised July 20, 2019

$$B_H(t) = \frac{KV_H^{\frac{1}{2}}}{\Gamma\left(H+\frac{1}{2}\right)}\left[\int_{-\infty}^{0}\left(|t-s|^{H-\frac{1}{2}} - |-s|^{H-\frac{1}{2}}\right)dB(s) + \int_{0}^{t}\left(|t-s|^{H-\frac{1}{2}}\right)dB(s)\right] \quad ...(1)$$

$$R_{B_H}(t_1,t_2) = \frac{1}{2}[|t_1|^{2H} + |t_2|^{2H} - |t_1-t_2|^{2H}] \quad ...(2)$$

$$R_{W_H}(\tau) = \frac{1}{2}[|\tau+1|^{2H} + |\tau-1|^{2H} - 2|\tau|^{2H}] \quad ...(3)$$

$$B_{H(t)}(t) = \frac{KV_{H(t)}^{\frac{1}{2}}}{\Gamma\left(H(t)+\frac{1}{2}\right)}\left[\int_{-\infty}^{0}\left(|t-s|^{H(t)-\frac{1}{2}} - |-s|^{H(t)-\frac{1}{2}}\right)dB(s) + \int_{0}^{t}\left(|t-s|^{H(t)-\frac{1}{2}}\right)dB(s)\right] \quad ...(4)$$

$$\lim_{\rho\to 0^+}\left[\frac{B_{H(t+\rho u)}(t+\rho u) - B_{H(t)}(t)}{\rho^{H(t)}}\right] = B_{H(t)}(u) \quad ...(5)$$

techniques are found to be useful for probing creep motion in glass beads when particles appear as a static solid [24]. Kang *et al*. have studied non-uniform flow behavior of fluidized particles using stochastic method [25].

This study presents a new statistical fractal approach to probe temporal dynamics of granular flow based multifractional Brownian motion (MBM). Time-varying Hurst exponent of the light intensity fluctuation will be used to characterize the transient as well as the stable state of the gravity driven quasi-two-dimensional granular flow.

2. Time-varying Fractal Stochastic Model

Fractal time series $X(t)$ satisfies scale invariance or self-similarity property, namely $X(at) \equiv a^{-H}X(t)$, where a is a scale factor with scaling exponent $0 < H < 1$. Here, the equivalence is in the sense of the probability distributions and it follows that key statistical properties such as the correlation function, variance and power spectral density exhibit power-law behavior.

One important and widely used fractal stochastic process with Gaussian probability distribution is the fractional Brownian motion (FBM) defined by [26] as presented in $Eq.(1)$ for $B_H(t)$. Where $0 < H < 1$ is the self-similar Hurst exponent and $B(t)$ is the Gaussian Brownian motion.

The multiplicative constant $V_H = \Gamma(2H+1)\cdot sin(\pi H)$ is normalizing factor so that $E\left[\left(B_H(1) - B_H(0)\right)^2\right] = K^2$, with K is a constant [27].

For a standard FBM when $K = 1$, $B_H(t)$ has zero mean with covariance $R_{B_H}(t_1,t_2)$ as shown in $Eq.(2)$.

Fractional Gaussian noise (FGN) $W_H(t)$is defined as the generalized derivative of FBM [26]. A discrete version represented as $W_H(t) \equiv B_H(t+1) - B_H(t)$is a stationary Gaussian process with zero mean and covariance given by $R_{W_H}(\tau)$ in $Eq.(3)$. As the lag $\tau \to \infty$, then $R_{W_H}(\tau) \sim H(2H-1)\cdot|\tau|^{2H-2}$. It follows from the covariance that FGN is uncorrelated for $H = 0.5$, hence corresponds to the standard Gaussian white noise. FGN is widely used for modelling stationary fractal noises with long-range correlation. FGN is said to be persistent when $\frac{1}{2} < H < 1$ and anti-persistent for $0 < H < \frac{1}{2}$.

While FBM and FGN have been tremendously useful for modelling fractal time series with constant scaling exponent H, they are not appropriate for characterizing transient or time dependent scaling behavior. A natural way to cater for this need is generalize the fractional Brownian motion with constant H to a process called multi fractional Brownian motion (MBM) with time-varying Hurst exponent $H(t)$. MBM was introduced independently by Peltier and Levy-Vehel [28] and Benassi *et al*. [29]. Following $Eq.(1)$, the moving average version of MBM is derived as $Eq.(4)$ presented by [28].

The deterministic multiplicative factor K' is assumed to be a slowly time-varying function and its estimation for empirical data is a non-trivial effort.

The sample paths of MBMs are locally asymptotically self-similar as represented via $Eq.(5)$ for $B_{H(t)}(u)$, where $B_{H(t)}(u)$ is FBM indexed by $H(t)$ and the equality is in the sense of distributions [29]. This property allows one to utilize many properties of FBM point-wise or in small time window τ as long as $\tau / t \to 0$.

$$X_{j+q} - X_j \sim N\left(0, K^2\left(\frac{q}{n-1}\right)^{2H(i)}\right) \quad ...(6)$$

$$S_{\delta,q}^k(i) = \frac{1}{(\delta - q + 1)} \sum_{j=i-\delta}^{i-q} \left|X_{j+q} - X_j\right|^k \quad ...(7)$$

$$H_{\delta,q}^k(i) = \frac{1}{k \log\left(\frac{q}{n-1}\right)} \log\left[\frac{\sqrt{\pi} S_{\delta,q}^k(i)}{2^{k/2}\Gamma\left(\frac{k+1}{2}\right) K^k}\right] \quad ...(8)$$

$$H_{\delta,q}^k(i) = \frac{1}{k \log\left(\frac{q}{n-1}\right)} \log\left[\frac{\sqrt{\pi} S_{\delta,q}^k(i)}{2^{k/2}\Gamma\left(\frac{k+1}{2}\right)}\right] - \frac{\log K}{\log\left(\frac{q}{n-1}\right)} \quad ...(9)$$

Next, we briefly describe the estimator for the discrete time-varying Hurst exponent, $H(i)$ following the technique developed by [27]. Suppose $\{X_i\}$, where $i = 1, \ldots, (n-1)$ is a discretized version of a MBM that locally behaves like a FBM as shown in $Eq.(6)$, where $j = i - \delta, \ldots, i - q$; $i = \delta + 1, \ldots, n$; $q = 1, \ldots, \delta$. The sum of k^{th} order moment of the increments is defined as $S_{\delta,q}^k(i)$ shown in $Eq.(7)$, where $i = \delta + 1, \ldots, n$. The estimator of $H(i)$ is then given by [27] as $H_{\delta,q}^k(i)$ shown in $Eq.(8)$ and $Eq.(9)$. For $K = 1$, i.e., when the time-series is not the standard MBM, then there exists a systematic bias in the estimation of local Hurst exponent shown in the last term of the right hand side of the $Eq.(9)$. For empirical time series, K is not known and thus need to be measured. The technique proposed in [27] uses the local properties of a subset of random variable $V_q = \{(X_{j+q} - X_j)\}$ such that the estimated H-exponent is constant within a fixed small radius ε, that is $H_{\delta,q}^k(i) \in (H - \varepsilon, H + \varepsilon)$ for $j = i - \delta, \ldots, i - q$; $i = \delta + 1, \ldots, n$. Because V_q is a normally distributed process with variance $K^2\left(\frac{q}{n-1}\right) \cdot 2H$, the factor K can be measured from the intercept of least square fitting of $\log var[V_q]$ versus $\log\left(\frac{q}{n-1}\right)$. Then again, we propose an unrefined however straight forward technique to estimate the bias term by 'stitching' a standardized fractional Brownian motion at the end of the original time-series and utilize this chunk of the data for re-adjusting the estimation of $H(i)$. Since $H = \frac{1}{2}$ or 0.5 is used as a benchmark, we derive the confidence interval for $H(i) = H = \frac{1}{2}$ by letting $k = 1$ and $q = 1$ in $Eq.(9)$ to get $\frac{1}{2} \pm \frac{z_\alpha}{2}\sqrt{var\left[H_{\delta,1}^1(i)\right]}$, with $\frac{z_\alpha}{2}$ is the standardized normal distribution at prediction level $100(1-\alpha)\%$.

A detailed discussion on the accuracy and Gaussianity test of the estimator can be found in [27]. However, we stress here that the choice of the window length δ should ensure that locally asymptotic normality (LAN) condition is satisfied so that MBM model requirements are met. In such circumstances, one may use the D'Agostino-Pearson test [30] that is based on the kurtosis and skewness estimations to verify the LAN condition, in this way making the MBM model valid. We adopt this method to get a rough estimate on optimal window length in order for LAN to be valid for all the time series. In order to improve the accuracy of the local Hurst exponent estimation, one may be tempted to increase the window length, hence reducing the estimator's variance and thus making $H(i)$ smoother. However, this will be at the expense of local characterization. For illustration, the sample paths of N_p -points standard MBM and its increments for a particular time-varying Hurst exponent, $H(t)$ namely are shown in Fig.1 for $N = 1024$. The simulation is done using the technique described in [28].

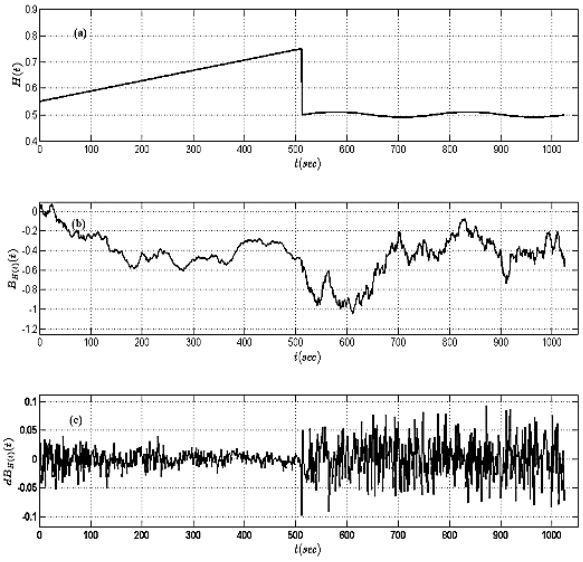

Fig.1. (a) An example of time-varying Hurst exponent and sample paths of (b) multi- fractional Brownian motion and (c) its increment process.

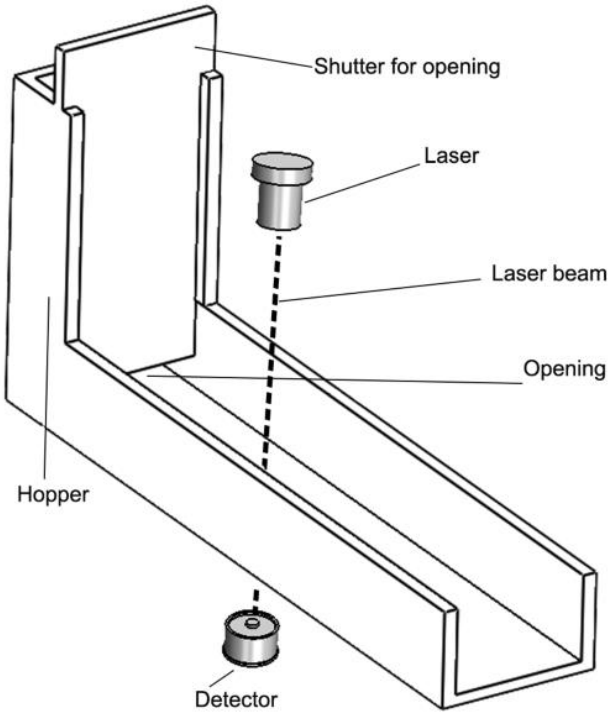

Fig.2. Experimental set-up for gravity-driven surface granular flow.

3. Light Scattering Experiment with Two-Dimensional Granular Flow

A simple setup for gravity-driven channel flow with vertical hopper is constructed as shown in Fig.2. The inclined channel is fabricated using 3 mm thick perplex glass sheets. The length and the width of channel are 80 cm and 15 cm, respectively. The opening of particle injector is controlled by movable shutter. The granular particles are dry, non-cohesive and mono disperse soda lime glass beads of sizes 4 mm , 6 mm and 8 mm in diameters, with the mean density of 2500 Kg/m^3. The beads are poured into a hopper reservoir connected at the top of inclined channel. The channel is inclined at 14° in all trials.

The hopper is connected to the channel inlet or entrance section with a rectangular plate of 15 cm by 40 cm. The opening width of entrance section is adjustable. We are also interested to study the influence of opening width on the granular flow transitions. Therefore, three different opening widths are set, namely 3-bead size width, 5-beads size width and 7-bead size width. We observed that there was no steady flow (but a jammed state) below 3-bead size width. Another plate of same dimension but slightly longer is inserted between the adjustable entrance plate and the channel to block the particles. We call this plate as a shutter for opening. After filling up the hopper, the shutter is pulled out very quickly and granular flows are begun by allowing particles to fall under the influence of the gravity. The total mass of the beads filling in the hopper is kept at a constant 2 Kg for all runs.

DLS techniques can be used to explore micro dynamics of three-dimensional granular packing. The experiment described here is however in quasi-2D system as the flow consists of one-bead thick layer of surface flow. Therefore, we introduce a modified version of speckle-visibility spectroscopy [31]. In this method, we transmit laser beam through the 2D granular bed instead of back-scattering as proposed by Dixon $et\ al.$ [31]. The initial beam of laser light diffuses through the flowing particles and forms an interference pattern known as speckle. These interference patterns carry whole information of inside of the sample. This technique is capable of resolving the evolution of microscopic dynamics throughout the course of a granular flow. DLS method is very sensitive to a small particle displacements (in the order of the wavelength of the light used). But, in our case, the size of particle is far greater than the wavelength of laser light. To solve this issue, we follow [32] to capture the inter-particle dynamics of even of larger particles.

A 3 mW polarized $He-Ne$ laser with wavelength of $\lambda = 636\ nm$ is used as the light source. The laser beam is expanded up to a few millimeters in diameter using a plano convex lens for illuminating a wider area for investigation. Intensity of scattered beam which transmitted through the surface granular flow is measured. Before focusing the beam onto a photo detector, Newport Photo diode 918D, scattered beam is first filtered from any ambient light using a bandpass filter and a polarizer. Signal from the photo detector is recorded using Newport $1936-C$ single channel optical power meter operating at the sampling rate of 10 kHz.

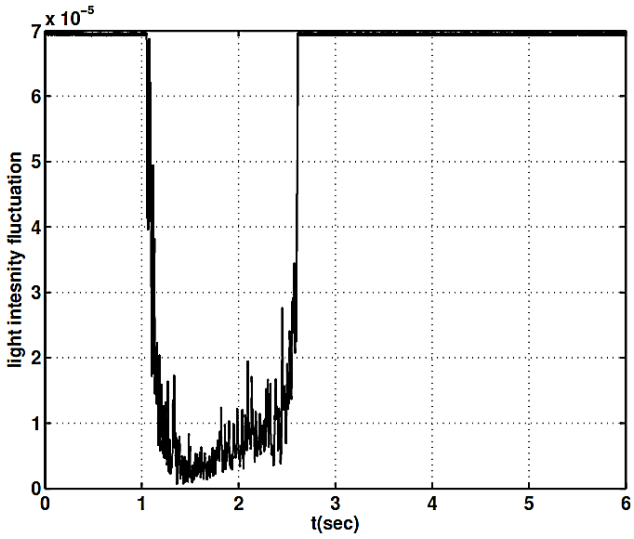

Fig.3. Typical light intensity fluctuation time series from Power Meter for flow of glass beads of $d = 6mm$ when shutter opening is set to 7-bead size.

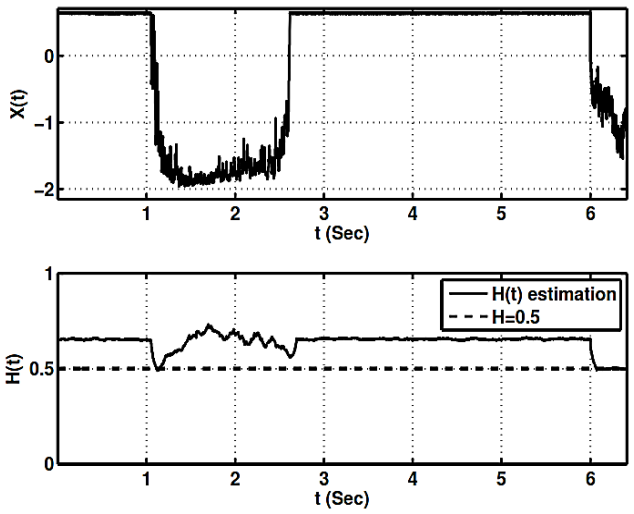

Fig.4. (Above): Normalized scattered light intensity time series of Fig.3. (Below): Hurst exponent of time series calculated using the method given in Section-2.

The whole experiment is carried out in an enclosure with minimum ambient light interference. A sample of the measured photodiode current corresponding to the light intensity fluctuation is shown in Fig.3. The flow experiments are repeated 5 times for each case i.e. different bead sizes and different hopper opening sizes. The light intensity fluctuation is normalized by subtracting its mean and dividing the de-mean time series by its standard deviation to allow easily comparison of the normalized intensity fluctuations. The time-varying Hurst exponent $H(t)$ is estimated for the normalized time series using $Eq.(8)$ as shown in Fig.4 [33][34][35][36][37][38].

4. Results and Discussion

Gravity-driven granular flow experiments were performed for two different cases, namely by (1) varying the bead diameters and (2) the opening size of the hopper. The light scattering intensity fluctuation were determined for three different bead diameters ($4\ mm$, $6\ mm$, $8\ mm$) and for each of these bead sizes, three different hopper opening sizes were tried (3 beads, 5 beads, 7 beads opening width).

Fig.5 shows the time series and the corresponding time-dependent Hurst exponents for granular flows of beads of different diameters for a fixed hopper opening width. Generally speaking, when the hopper opening width is increased, the density of beads in channel is also increased which changes the overall flow behavior. For smaller opening entrance, lesser particles are flown in the channel and the fluctuation pattern behaves Brownian motion with Hurst exponent closer to 0.5. This behavior is observed for hopper opening width of three beads diameter as shown in Fig.5(a). If shutter opening is increased further, the fluctuation becomes more regular with Hurst exponents greater than 0.5 as seen in Fig.5(b) and in Fig.5(c) for opening width of 5-beads and 7-beads, respectively.

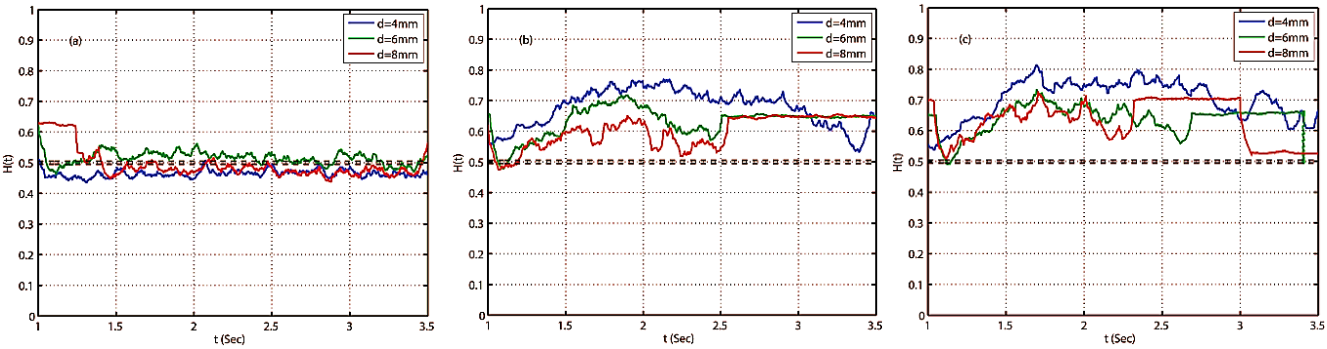

Fig.5. (Color online) $H(t)$ estimation for same opening size of shutters while the diameter of particles is varied. The opening shutter is (a) 3-bead size, (b) 5-bead size, and (c) 7-bead size.

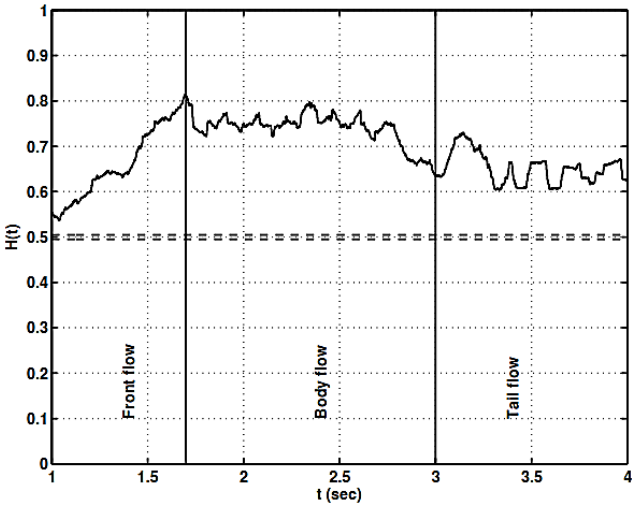

Fig.6. Curve is divided into three sections according to arrival and departure of particles in channel. Fluctuation in H-exponent correlates the phases of flow.

We noticed that the variation of Hurst exponent can also provide evidence for qualitative description of the flow state. Based on Fig.6, there appears to be a general trend in the $H(t)$ plots over time for larger hopper opening widths. We can roughly classify the flow into three temporal regimes, namely the initial transient front (head), followed by the steady state flow (body) and finished by the residual transient flow (tail). For the flow front regime, the Hurst exponent increases (from irregular to more regular fluctuation), before settling to steady flow with approximately constant Hurst exponent. During the tail flow, the residual particles produce intense fluctuation, hence the drop in the Hurst exponent values. In Fig.7, we show the $H(t)$ plots drawn for fixed bead diameter but different hopper opening widths. Flow characteristics do not change very much for larger hopper openings (5 beads and 7 beads), and the trend is maintained for the 3 bead diameters considered here.

5. Conclusion

We have described the use of light scattering intensity fluctuation and fractal stochastic process with time-varying Hurst exponent, namely multi fractional Brownian motion to characterize granular flow states. The technique can be adopted as a combined probe to other visualization approaches to study granular flow. Intensity fluctuation is found to corroborate well with the flow development over time. The time-varying Hurst exponent were used to determine three different regimes, denoted as front, body and tail flows. The flow characteristics were found to be less affected by larger hopper openings (5 beads and 7 beads). It is suggested that the time-varying fractals may be useful for modelling (audio) signals generated by landslides or avalanche.

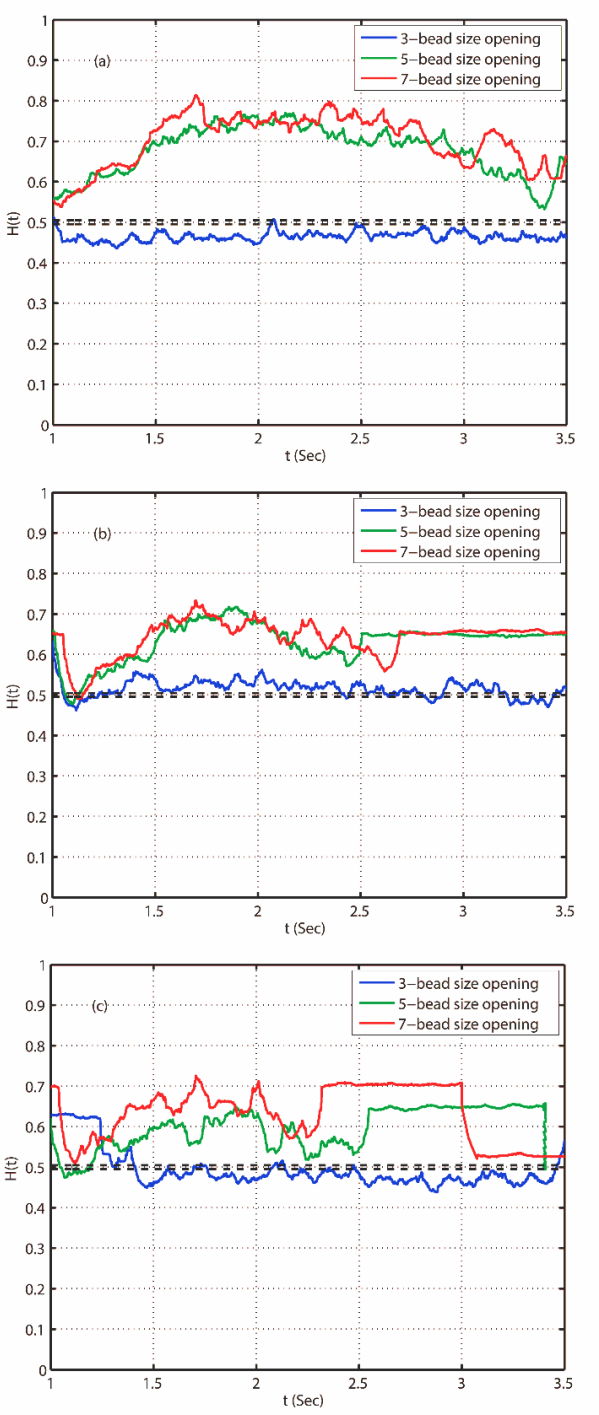

Fig.7. (Color online) Fluctuation in H-exponent for same bead diameter as a function of size of opening entrance:
(a) $d = 4mm$, (b) $d = 6mm$, and (c) $d = 8mm$.

Acknowledgement

The authors pay thanks to the Malaysian Ministry of Education for funding support under Fundamental Research Grant Scheme ($FP057-2014A$) and University of Malaya for research grants ($UMRG: RG231-12AFR$ and $BKP: BK002-2014$).

References

[1] A. J. Liu, S. R. Nagel, Nonlinear dynamics: Jamming is not just cool any more, Nature 396 (1998) 21–22.

[2] P. Jop, Y. Forterre, O. Pouliquen, A constitutive law for dense granular flows, Nature 441 (2006) 727–30.

[3] T. S. Majmudar, M. Sperl, S. Luding, R. P. Behringer, Jamming transition in granular systems, Physical Review Letters 98 (2007) 058001–4.

[4] R. Bureau, S. Brand, R. C. Ball, M. Nicodemi, Flow regimes of a fluid driven granular suspension, Granular Matter 14 (2012) 175–178.

[5] R. Chand, M. A. Khaskheli, A. Qadir, B. Ge, Q. Shi, Discrete particle simulation of radial segregation in horizontally rotating drum: Effects of drum-length and non-rotating end-plates, Physica A 391 (2012) 4590–4596.

[6] T. Borzsonyi, R. E. Ecke, Rapid granular flows on a rough incline: Phase diagram, gas transition, and effects of air drag, Physical Review E 74 (2006) 061301–9.

[7] S. Savage, The mechanics of rapid granular flows, Advances in Applied Mechanics 24 (1984) 289–366.

[8] J. Zhong, M. Hou, Q. Shi, K. Lu, Criticality of the dilute-to-dense transition in a 2d granular flow, Journal of Physics: Condensed Matter 17 (2006) 2789–2794.

[9] G. G. Zhou, Q. Sun, Three-dimensional numerical study on flow regimes of dry granular flows by dem, Powder Technology 239 (2013) 115–127.

[10] H. J. Herrmann, J. P. Hovi, S. Luding, Physics of Dry Granular Media, no. NATO ASI Series E, Kluwer Academic Publishers, Dordrecht, (1998).

[11] G. C. Yang, Q. Y. Liu, M. B.Hu, R. Jiang, Q. S. Wu, Phase transition and bistable phenomenon of granular flows down a chute with successive turnings, Physics Letters A 378 (2014) 1281–1285.

[12] P. C. Johnson, P. Nott, R. Jackson, Frictional-collisional equations of motion for participate flows and their application to chutes, Journal of Fluid Mechanics 210 (1990) 501–535.

[13] C. Ancey, Dry granular flows down an inclined channel: Experimental investigations on the frictional-collisional regime, Physical Review E 65 (2011) 011304–19.

[14] K. To, P. Y. Lai, H. K. Pak, Jamming of granular flow in a two-dimensional hopper, Physical Review Letters 86 (2001) 71–74.

[15] V. Kumaran, S. Maheshwari, Transition due to base roughness in a dense granular flow down an inclined plane, Physics of Fluids 24 (2012) 053302.

[16] Y. G. Drake, Granular flow: physical experiments and their implications for microstructural theories, Journal of Geophysical Research: Solid Earth 225 (1991) 121–152.

[17] T. G. Drake, Structural features in granular flows, Journal of Fluid Mechanics 95 (1990) 8691–8696.

[18] E. Azanza, F. Chevoir, P. Moucheront, Experimental study of collisional granular flows down an inclined plane, Journal of Fluid Mechanics 400 (1999) 199–227.

[19] M. Hou, W. Chen, T. Zhang, K. Lu, Global nature of dilute-to-dense transition of granular flows in a 2d channel, Physical Review Letters 91 (2003) 204301–4.

[20] DeGennes, P. G., J. Duran, and A. Reisinger. "Sands, Powders, and Grains: An Introduction to the Physics of Granular Materials (Partially Ordered Systems)." (2000).

[21] K. Kima, H. K. Pak, Diffusing-wave spectroscopy study of microscopic dynamics of three dimensional granular systems, Soft Matter 6 (2010) 2894–2900.

[22] N. Menon, D. Durian, Diffusive-wave spectroscopy of dynamics in a three-dimensional granular flow, Science 5308 (1997) 1920–1922.

[23] S. S. Safaai, S. V. Muniandy, W. X. Chew, H. Asgari, S. L. Yap, C. S. Wong, Fractal dynamics of light scattering intensity fluctuation in dis- ordered dusty plasma, Physics of Plasma 20 (2013) 103702–8.

[24] L. Djaoui, J. Crassous, Probing creep motion in granular materials with light scattering, Granular Matter 7 (2005) 185–190.

[25] Y. Kang, K. L. Woo, M. H. Ko, Y. J. Cho, S. D. Kim, Particle flow behavior in three-phase fluidized beds, Korean J. Chem. Eng. 16 (6) (1999) 784–788.

[26] B. B. Mandelbrot, The Fractal Geometry of Nature, W. H. Freedman and Co., New York, (1983).

[27] S. Bianchi, Pathwise identification of the memory function of multi fractional brownian motion with application to finance, International Journal of Theoretical and Applied Finance 8 (2) (2005) 255–281.

[28] R.-F. Peltier, J. L. Vehel, Multifractional brownian motion: definition and preliminary results, INRIA Technical Report RR-2645. [Accessed: 2019]

[29] A. Benassi, S. Jaffard, D. Roux, Gaussian processes and pseudo-differential elliptic operators, Revista Matematica Iberoamericana 13 (1) (1997) 19–89.

[30] R. B. D'Agostino, A. B. J. R. B. D'Agostino, A suggestion for using powerful and informative tests of normality, American Statistician 44 (1990) 316–321.

[31] P. Dixon, D. Durian, Speckle visibility spectroscopy and variable granular fluidization, Phys. Rev. Lett. 90 (18) (2003) 84302–4.

[32] G. Caballero, E. Kolb, A. Lindner, J. Lanuza, E. Clement, Experimental investigation of granular dynamics close to the jamming transition, J. Phys.: Condens. Matter 17 (2005) S2503–S2516.

[33] H. Saleem, A. H. Nizamani, W. A. Bhutto, A. M. Soomro, M. Y. Soomro, A. Toufik, "Two Dimensional Natural Convection Heat Losses from Square Solar Cavity Receiver," IJCSNS International Journal of Computer Science and Network Security, vol. 19, no. 4, (2019).

[34] M. Y. Channa, A. H. Nizamani, H. Saleem, W. A. Bhutto, A. M. Soomro and M. Y. Soomro, "Surface Ion Trap Designs for Vertical Ion Shuttling," IJCSNS International Journal of Computer Science and Network Security, vol. 19, no. 4, (2019).

[35] A. M. Soomro, W. A. Bhutto, A. H. Nizamani, H. Saleem, M. Y. Soomro, M. A. Khaskheli, N. M. Shaikh, "Controllable Growth of Hexagonal BN Monolayer Sheets on Cu Foil by LPCVD," IJCSNS International Journal of Computer Science and Network Security, vol. 19, no. 6, (2019).

[36] M. Y. Channa, A. H. Nizamani, A. M. Soomro, H. Saleem, W. A. Bhutto, M. Y. Soomro, M. A. Khaskheli, and N. M. Shaikh, "Vertical Ion Shuttling Protocols for Multi-Strip Surface Ion Traps," IJCSNS International Journal of Computer Science and Network Security, vol. 19, no. 7, (2019).

[37] H. Saleem & et al., "Imposing Software Traceability and Configuration Management for Change Tolerance in Software Production," IJCSNS International Journal of Computer Science and Network Security, vol. 19, no. 1, (2019).

[38] H. Saleem & et al., "Novel Intelligent Electronic Booking Framework for E-Business with Distributed Computing and Data Mining," IJCSNS International Journal of Computer Science and Network Security, vol. 19, no. 4, (2019).